JBAT 15(1) (2026) 42 – 53

Jurnal Bahan Alam Terbarukan

p-ISSN 2303 0623
e-ISSN 2407 2370

Accredited SINTA 3 by Ministry of Research and Technology/National Research and Innovation Agency
SK No. 10/C/C3/DT.05.00/2025
http://journal.unnes.ac.id/nju/index.php/jbat

Enhanced Photocatalytic Degradation of Methyl Orange Using N-Doped Carbon Quantum Dots/TiO_2 Nanocomposite Derived from Orange Peel

Muhammad Adam Purnawan[1], Shaka Kusuma Nurjati[1], Faatin Nisriinaa Zain[1], Fakhri Ahmad Kurniawan[2], Maulida Zakia[1,✉]

DOI: https://doi.org/10.15294/jbat.v15i1.35263

[1]Department of Chemical Engineering, Faculty of Engineering, Universitas Negeri Semarang, Sekaran Campus, Semarang 50229, Indonesia
[2]Department of Environmental Science, Faculty of Mathematics and Natural Sciences, Universitas Negeri Semarang, Sekaran Campus, Semarang 50229, Indonesia

Article Info

Article history:
Received
12 January 2026
Revised
25 March 2026
Accepted
30 May 2026
Published
June 2026

Keywords:
Degradation;
Methyl orange;
Quantum dots;
TiO_2 NPs;
Orange peel;
Photocatalyst

Abstract

The release of azo dyes such as Methyl Orange (MO) from the textile industry poses serious environmental problems due to their toxic, stable, and difficult-to-degrade properties. Conventional treatment methods such as adsorption, coagulation, and chemical oxidation have not been able to effectively degrade dyes, so a more efficient and environmentally friendly alternative approach is needed. Photocatalysis technology is a potential solution because it can mineralize organic compounds into harmless products. However, conventional photocatalysts such as TiO_2 NPs have limited activity in visible light due to their large band gap and high electron-hole recombination rate. This study aims to improve the photocatalytic performance of TiO_2 NPs through the integration of nitrogen-doped carbon quantum dots (NCQDs) synthesized from orange peel waste using a one-step hydrothermal carbonization method, then composited with TiO_2 NPs through a low-temperature hydrothermal reaction. Characterization was performed using SEM and SEM-EDX to analyze the morphology and elemental composition. Photocatalytic activity was tested against MO degradation under UV irradiation using a UV-Vis spectrophotometer. The results showed that the NCQDs/TiO_2 composite had a homogeneous morphology and strong chemical interaction between NCQDs and TiO_2 NPs. Degradation efficiency reached 32.5% in 90 minutes, higher than pure TiO_2 NPs by 2.5%, with an increase in the reaction rate constant from 2.81×10^{-4} to 4.37×10^{-3} min^{-1} and a decrease in half-life from 41.1 h to 2.65 h. Thus, the NCQDs/TiO_2 nanocomposite based on orange peel has potential as a sustainable photocatalyst for the treatment of MO.

INTRODUCTION

The textile industry's production of fiber, yarn, and fabric-based materials heavily relies on the use of dyes. Globally, more than 70 million tons of synthetic dyes are produced annually, with nearly 50% consisting of azo dyes. Inefficient textile dyeing processes lead to the discharge of 15–50% of these dyes into wastewater, equivalent to approximately 280,000 tons released into the environment each year. As a result, textile dye effluents are estimated to account for 17–20% of global water pollution, making them one of the most significant contributors to industrial contamination (Dutta et al., 2024). However, these commonly used dyes have the potential to become hazardous waste that can pollute the environment (Alardhi et al., 2023). Azo dyes, particularly Methyl Orange (MO), are widely used in various industrial sectors such as textiles, food, pharmaceuticals, laboratories, and cosmetics due to their high chemical stability (Nazir et al., 2024;

✉ Corresponding author:
E-mail: maulida.zakia@unnes.ac.id

Peerakiatkhajohn et al., 2021). MO is a hazardous pollutant that is difficult to degrade because of its azo group (–N=N–). Even at low concentrations, it can cause toxic effects such as irritation, genetic mutations, disruption of aquatic ecosystems, and bioaccumulation in the food chain. Therefore, it requires safe treatment before being discharged into the environment (Emmanuel et al., 2023). Various conventional methods have been applied to remove dyes from wastewater, such as coagulation, chemical oxidation, membrane separation, solvent extraction, and adsorption (Lan et al., 2022). However, MO is difficult to degrade using these conventional methods, which instead risk causing pollutant accumulation (Aljuaid et al., 2023). On the other hand, photodegradation offers advantages such as a simple process, environmental friendliness, cost-effectiveness, effectiveness in reducing pollutant concentrations to ppm/ppb levels, and the ability to mineralize pollutants without producing harmful by-products (Khan et al., 2020).

Carbon quantum dots (CQDs) are promising semiconductor nanomaterials for photocatalytic applications due to their environmentally friendly nature, low toxicity, good biostability, high water solubility, and low production cost (Cui et al., 2021). The utilization of CQDs is a relatively new method and has not yet been widely applied, but its scientific appeal has been globally recognized through the 2023 Nobel Prize in Chemistry. CQDs can be produced via a one-step synthesis process based on low-temperature hydrothermal methods (Aslan et al., 2023; Surendran et al., 2020). This method is chosen because it is environmentally friendly, energy-efficient, and produces carbon materials with diverse properties (Nazibudin et al., 2023). Previous studies have shown the effectiveness of carbon quantum dots in photocatalysis. For example, nitrogen-doped CQDs synthesized from watermelon rind via a simple hydrothermal method were reported to achieve nearly 69% degradation of MO within 120 minutes under visible light irradiation, attributed to their small particle size, high surface area, and abundant oxygen-containing functional groups (Remli & Aziz, 2020). This proves that CQDs can also be made using alternative agricultural waste biomass without using chemicals to reduce environmental pollution (Sadeghi-chahnasir et al., 2024).

On the other hand, in real-world contexts, orange peel waste is an agricultural biomass that has not been utilized effectively. Global orange production exceeds 72 million tons per year, and the processing of this fruit generates approximately 25 million tons of waste worldwide, primarily consisting of inedible parts such as peels and seeds. Orange peels alone account for 50–70% of this total waste, making them a major contributor to organic agricultural waste (Tahir et al., 2023). Orange peels contain cellulose, hemicellulose, amino acids, and bioactive compounds such as polyphenols and flavonoids, making them an ideal carbon source for the synthesis of CQDs with superior optical and photoluminescent properties (Olmos-Moya et al., 2022).

Similar existing research has demonstrated the integration of carbon quantum dots (CQDs), titanium dioxide nanoparticles (TiO_2 NPs), and nitrogen (N) doping. CQDs are known for their high fluorescence, biocompatibility, and good conductivity, enabling them to absorb light and transfer electrons, but they are not sufficiently robust to act as the primary photocatalyst (Mei et al., 2022). TiO_2 NPs is a widely used photocatalytic material due to its stability and abundant availability, but it is limited by its wide bandgap (~3.2 eV), making it active only under ultraviolet light (Zhang et al., 2022). Nitrogen doping has been proven to lower the bandgap energy of TiO_2 NPs, enhance visible light absorption, and accelerate charge transfer and electron-hole pair separation. A study by Khan et al. (2020) showed that nitrogen doping can reduce the bandgap of TiO_2 NPs to 2.95 eV, while Karaca et al. (2023) reported an increase in organic pollutant degradation efficiency to nearly 98% using N-CQDs/TiO_2 nanocomposites. However, previous research still uses environmentally unfriendly inorganic materials as a source of CQDs, as well as multi-step synthesis methods that are impractical and expensive. In addition, there have not been many studies that explicitly combine the three elements of CQDs, N, and TiO_2 NPs in a single direct synthesis process.

Therefore, the solution that will be achieved is to utilize orange peel biomass as a precursor for the synthesis of nitrogen-doped CQDs through a one-step synthesis approach in the hydrothermal carbonization process. The synthesized CQDs are then directly composited with TiO_2 NPs, forming an NCQDs/TiO_2 structure that can broaden the light absorption spectrum,

reduce the bandgap, and suppress charge recombination.

MATERIALS AND METHOD

Materials

The oranges used in this study were Citrus reticulata obtained from local vendors in the Semarang area, deionized water (ONELAB, Indonesia), 0.1 M H_2SO_4 (Merck, Germany), 9% NaClO, 70% ethanol (ONEMED, Indonesia), 99% research grade TiO_2 NPs (ITNANO, Indonesia), and methyl orange.

Equipments

The equipment used in this study included an oven (Memmert UN55, Germany), hydrothermal reactor, centrifuge, sonicator (JP-040S, Manufacture Expert, China), UV lamp (6W, Vilber Lourmat), and Whatman No. 42 filter paper. For characterization, a UV-Vis spectrophotometer (UH5300, Japan) and Scanning Electron Microscope (Phenom Pro X Dekstop) with an Energy Dispersive X-ray (EDX) unit were used.

Method

Preparation of N-Doped Orange Peel-Based CQDs

The preparation of nitrogen-doped carbon quantum dots (NCQDs) began with washing the orange peel, drying it in the sun, and grinding it using a blender. Next, the orange peel is dried in an oven at 150 °C for 10 h. Then, 4 g of orange peel is washed in 100 mL of 0.1 M H2SO4 solution, followed by filtration and rinsing with deionized water until the pH reaches 7. The orange peel is then dried in an oven at 150°C for 2 h. The orange peel is mixed with 60 mL of 9% NaClO solution and stored at room temperature for 4 h, followed by filtration and rinsing with distilled water until the pH reaches 7. The orange peel is then stored in a desiccator.

Production of NCQDs

2.67 grams each of orange peel and urea were placed in 40 mL of deionized water and sonicated for 30 minutes. The solution was then placed in an autoclave and oven-dried at 180°C for 12 h for hydrothermal carbonization. The autoclave was allowed to cool naturally, then the solution was centrifuged at 4000 rpm for 30 minutes to separate the suspension from the supernatant. The NCQDs suspension was then dried at 100°C for 2 h.

Synthesis of NCQDs with TiO_2 NPs

The synthesis process of NCQDs/TiO_2 begins with the addition of TiO_2 NPs (20, 40, and 60 mg) to 40 mL of NCQDs suspension solution (400 mg/L). The suspension was sonicated for 30 minutes, then placed in an autoclave at 150°C for 12 h. Next, the product was centrifuged at 4000 rpm and followed by centrifugal washing using deionized water and ethanol. NCQDs/TiO_2 was separated from the supernatant and stored in a desiccator.

Characterization of N-Doped CQDs with TiO_2 NPs

The NCQDs/TiO_2 samples were then characterized. The morphology was observed using Scanning Electron Microscopy (SEM) and Energy Dispersive X-Ray Spectroscopy (EDX) for NCQDs/TiO_2.

Study of the Photocatalytic Activity of N-Doped CQDs with TiO_2 NPs

The photocatalytic activity was evaluated by the degradation of MO dye and monitored by a UV-Vis spectrophotometer over a period of 50 min at 10 min intervals. Degradation efficiency (%) is based the following Eq. 1.

$$\text{Degradation (\%)} = \frac{C_0 - C}{C_0} \times 100 \qquad (1)$$

Where C_0 represent initial concentration of the MO solution (mg/L), and C represents the concentration of the MO solution after a certain degradation period (mg/L).

RESULT AND DISCUSSION

The synthesis scheme of NCQDs/TiO_2 nanocomposites is summarized visually in Figure 1. to provide an overview of the manufacturing stages. The process begins with the pre-treatment of orange peel waste, followed by hydrothermal carbonization with urea to form NCQDs, and ends with the immobilization of TiO_2 NPs on the surface of NCQDs.

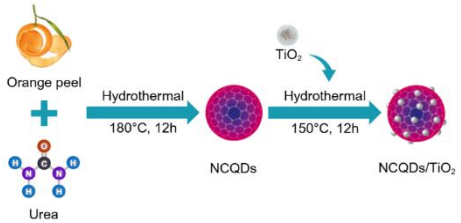

Figure 1. Schematic of the synthesis of NCQDs/TiO_2 nanocomposites from orange peel

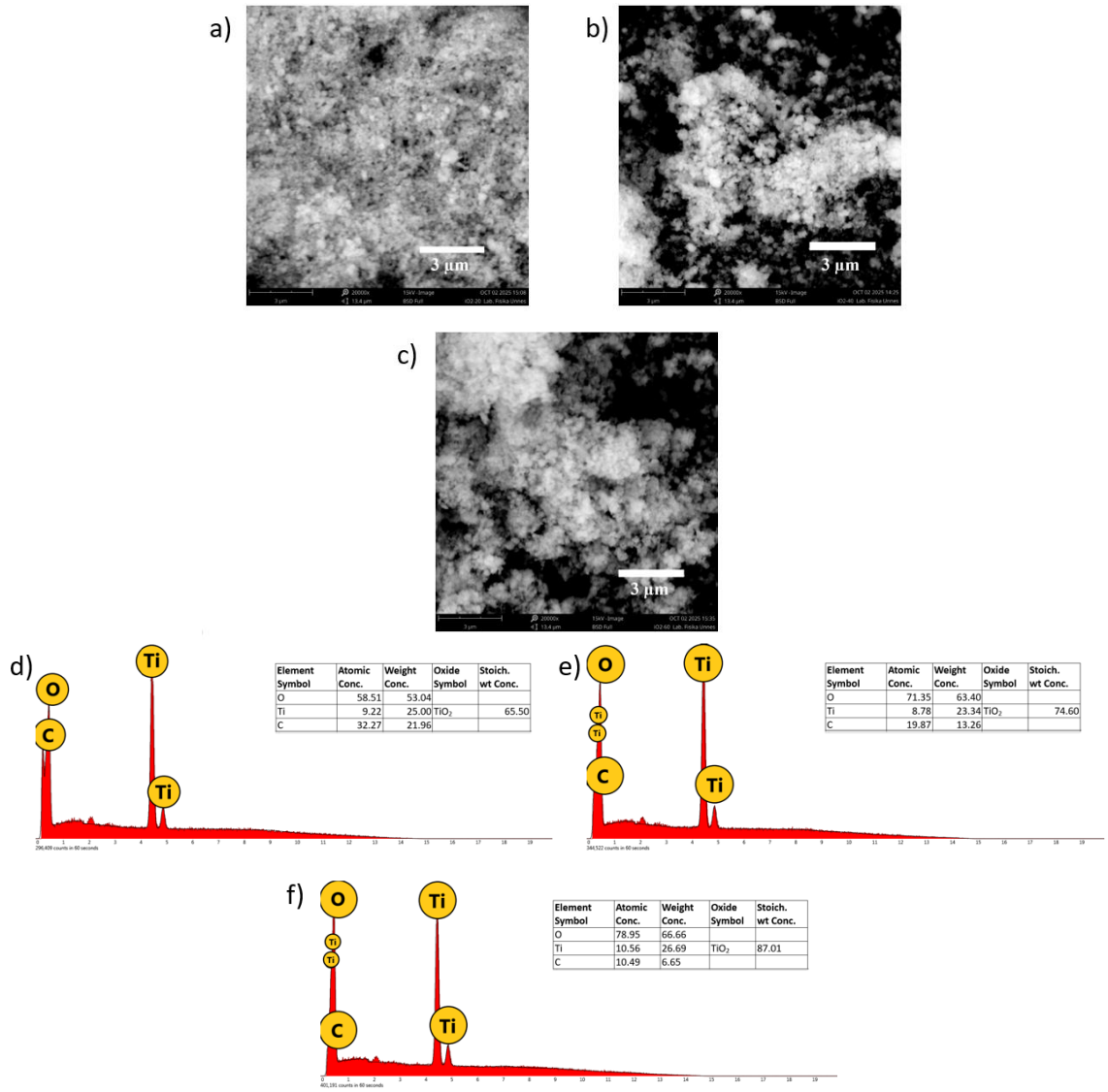

Figure 2. SEM image of NCQDs/TiO_2 NP concentrations of: (a) 20 mg; (b) 40 mg; and (c) 60 mg; EDX images of NCQDs/TiO_2 with TiO_2 NPs concentrations of: d) 20 mg; e) 40 mg; and f) 60 mg

After production, the NCQDs/TiO_2 nanocomposites were characterized morphologically using SEM. The results are shown in Figure 2.

Figure 2(a–d) presents the SEM images of NCQDs/TiO_2 nanocomposites synthesized with different TiO_2 NPs concentrations (20, 40, and 60 mg) and a control sample without TiO_2 NPs. Based on the characterization results, significant morphological phenomena and element distribution were observed. At 20 mg TiO_2 NPs (Figure 2a), the nanocomposite surface appears relatively homogeneous and fine-textured, with TiO_2 NPs evenly distributed within the NCQDs matrix. This morphology indicates a good interfacial contact and successful immobilization of TiO_2 NPs on the NCQDs surface, which enhances light absorption and provides abundant active sites for photocatalytic reactions (Immanuvel et al., 2024). Increasing the TiO_2 NPs consentration to 40 mg (Figure 2b), the formation of larger particle clusters and slight agglomeration result from excessive TiO_2 NPs particles that limit the dispersion of NCQDs. This behaviour is consistent with the coalescence phenomenon commonly observed in nanocomposites, which can be promoted by interfacial surface tension between nanoparticles. Such aggregation reduces the effective surface area and active sites, thereby slightly decreasing the photocatalytic efficiency (Malitha et al., 2024). Although agglomeration reduces the specific surface area, the interparticle

contact can still promote electron transfer between TiO_2 and NCQDs. At 60 mg TiO_2 NPs (Figure 2c), significant particle agglomeration and irregular clusters are observed. The dense structure may hinder light penetration and reduce photocatalytic efficiency due to charge recombination. This indicates that the 20 mg TiO_2 sample exhibits the most optimal interaction between NCQDs and the TiO_2 NPs matrix, forming a stable hybrid structure with a high number of active sites (Prabhakaran et al., 2025). Conversely, at 40 mg and 60 mg TiO_2 NPs, there was an increase in particle agglomeration, visible as clumps in the SEM image. This phenomenon was caused by an excess of TiO_2 NPs mass that was not evenly distributed in the NCQDs matrix, thus tending to form bonds between the TiO_2 NPs particles themselves (Harunrasjid et al., 2023).

SEM-EDX characterization was carried out to further confirm the elemental composition and successful formation of the NCQDs/TiO_2 nanocomposite. The EDX results (Figure 2e-h) clearly demonstrate the presence of titanium (Ti), oxygen (O), and carbon (C) elements, which are the main constituents of TiO_2 NPs and NCQDs. The detection of these three elements strongly indicates that the synthesis process successfully incorporated NCQDs onto the TiO_2 NPs surface. The varying atomic and weight concentrations among samples with different TiO_2 NPs loadings reflect the influence of TiO_2 NPs content on the surface composition and dispersion behavior of NCQDs.

In Figure 2(e), corresponding to the NCQDs/TiO_2 composite synthesized with a TiO_2 nanoparticle concentration of 20 mg, the EDX spectrum displays pronounced peaks for both O and C elements along with two distinct Ti peaks. Although the Ti signal is clearly visible in the spectrum, its atomic concentration (9.22%) remains lower compared to O (58.51%) and C (32.27%), indicating that TiO_2 is well-dispersed but not dominant on the composite surface. The relatively high carbon content implies that NCQDs were effectively anchored onto the TiO_2 NPs surface, forming a uniform interface between the carbonaceous and oxide phases. The detection of Ti and O further verifies the retention of TiO_2 NPs as the primary structural framework of the composite. These findings are consistent with previous studies, where Li et al. (2018) and Yang et al. (2018) reported that the incorporation of carbon-based quantum dots onto TiO_2 NPs led to a slight increase in carbon composition compared to pristine TiO_2 (from 1.94% to 2.13%). Their HRTEM analysis further confirmed the successful deposition of CQDs on the TiO_2 surface, with lattice spacings of 0.35 nm and 0.24 nm corresponding to the (101) plane of anatase TiO_2 NPs and the CQD lattice, respectively (Mahmood et al., 2021). The coexistence of these planes within the same region provided clear evidence of strong interfacial interaction between the carbon and oxide phases, which aligns with the elemental distribution observed in this study.

In Figure 2(f), which represents the sample with a TiO_2 NPs concentration of 40 mg, a distinct shift in elemental proportion is observed. The oxygen concentration increases significantly to 71.35%, while carbon decreases to 19.87%, and Ti remains moderate at 8.78%. The stronger O peak and weaker C signal indicate that TiO_2 NPs have begun to dominate the surface morphology. This phenomenon may be attributed to the partial agglomeration of TiO_2 at higher concentrations, which limits the exposure of NCQDs on the composite surface and reduces their uniform distribution (Malitha et al., 2024). The presence of oxygen-containing surface groups on TiO_2 facilitates the nucleation of carbon quantum dots during hydrothermal synthesis, which enhances carbon anchoring and improves interfacial interaction (Song et al., 2022). Consequently, even though Ti and O are still strongly detected, the decreased C signal suggests that carbon quantum dots are not uniformly distributed, which can negatively affect the nanocomposite's optical and electronic properties.

In Figure 2(g), corresponding to the 60 mg TiO_2 NPs sample, the trend becomes more pronounced. The EDX analysis reveals that oxygen and titanium are the dominant elements, with atomic concentrations of 78.95% and 10.56%, respectively, while carbon drastically drops to only 10.49%. This result signifies that excessive TiO_2 NPs concentration leads to pronounced nanoparticle agglomeration, which covers the NCQD layer and prevents uniform coating. The thick TiO_2 NPs aggregation not only limits the number of surface-active sites for carbon interaction but also inhibits light penetration into NCQDs, potentially decreasing photocatalytic efficiency. This observation is consistent with reports by Wang et al. (2022), who found that excessive TiO_2 NPs loading can cause self-shielding effects that hinder

charge transfer processes. Therefore, at this concentration, the NCQDs–TiO_2 interface becomes inefficient, and the structural integrity of the nanocomposite is compromised. Comparatively, as the TiO_2 NPs concentration increases from 20 mg to 60 mg, a consistent decrease in carbon content and a simultaneous increase in oxygen and titanium peaks are observed. This trend demonstrates that higher TiO_2 NPs loading leads to stronger oxide dominance and reduced carbon exposure on the surface. Consequently, the optimal interaction between NCQDs and TiO_2 NPs occurs at the lowest TiO_2 NPs concentration (20 mg), where the interface formation is the most effective and the carbon content remains high.

To investigate the optical properties of the synthesized materials and confirm the electronic interactions between the components, UV-Vis absorption spectroscopy was performed. The spectra of pristine NCQDs and the NCQDs/ TiO_2 composites with varying TiO_2 NPs loads (20, 40, and 60 mg) are presented in Figure 3.

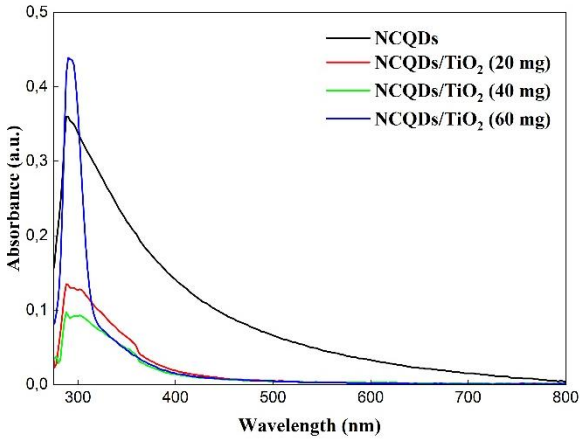

Figure 3. UV-Vis absorption spectra of NCQDs and NCQDs/TiO_2 composites synthesized with varying TiO_2 NPs mass loadings (20, 40, and 60 mg).

The pristine NCQDs (black line) exhibit a characteristic broad absorption spectrum. A distinct peak is observed at 285 nm, which can be attributed to the $\pi \rightarrow \pi^*$ transitions of the C=C bonds within the graphitic carbon core (Immanuel et al., 2024). Furthermore, a prominent absorption tail extends across the entire visible light region (400–800 nm). This broad absorption is a key feature of NCQDs, originating from various surface states and functional groups, and it endows the material with significant visible-light-harvesting capabilities (Prabhakaran et al., 2024).

Upon the incorporation of TiO_2 NPs, a significant change in the optical properties is observed. All composite samples (NCQDs/TiO_2 20, 40, and 60 mg) demonstrate a substantial suppression, or quenching, of the characteristic NCQD absorbance across both the UV and visible regions. This phenomenon is a strong indicator of effective electronic coupling between the NCQDs and the TiO_2 NPs. Instead of a simple additive spectrum, the observed quenching suggests a rapid non-radiative decay pathway, likely the efficient transfer of photogenerated charge carriers (electrons or holes) at the newly formed heterojunction interface (Xie et al., 2018). This interaction effectively quenches the intrinsic optical transitions of the NCQDs, which is a hallmark of a well-formed composite system and is highly beneficial for photocatalysis as it implies the initial step of charge separation (putro et al., 2018).

A clear trend is discernible with increasing TiO_2 NPs concentration. The composite with 60 mg of TiO_2 NPs (blue line) shows the most dramatic change. Its spectrum is dominated by a sharp, intense absorption peak below 300 nm, which is characteristic of the band-gap absorption of anatase TiO_2 NPs (Harunrasjid et al., 2023). The broad visible light absorption tail associated with the NCQDs is almost completely eliminated. This suggests that at such a high loading, the TiO_2 nanoparticles likely aggregate (as supported by SEM analysis) and "shield" the NCQDs, causing the overall optical properties to be dominated by TiO_2 NPs rather than the synergistic composite.

In contrast, the NCQDs/TiO_2 (20 mg) composite (red line) represents an optimal balance. While it exhibits significant quenching, confirming strong interfacial contact and charge transfer potential, it simultaneously retains a more pronounced absorption tail in the visible region compared to both the 40 mg (green line) and 60 mg samples.

This finding is critical and aligns perfectly with the SEM-EDX results. The 20 mg sample, which showed the most homogeneous dispersion of TiO_2 NPs, facilitates the formation of a maximum number of effective heterojunctions. This leads to the observed quenching (indicative of charge separation) without completely sacrificing the vital visible-light-harvesting ability of the NCQDs. The 40 mg and 60 mg samples, likely suffering from particle aggregation, exhibit less favorable optical properties for visible-light-driven photocatalysis.

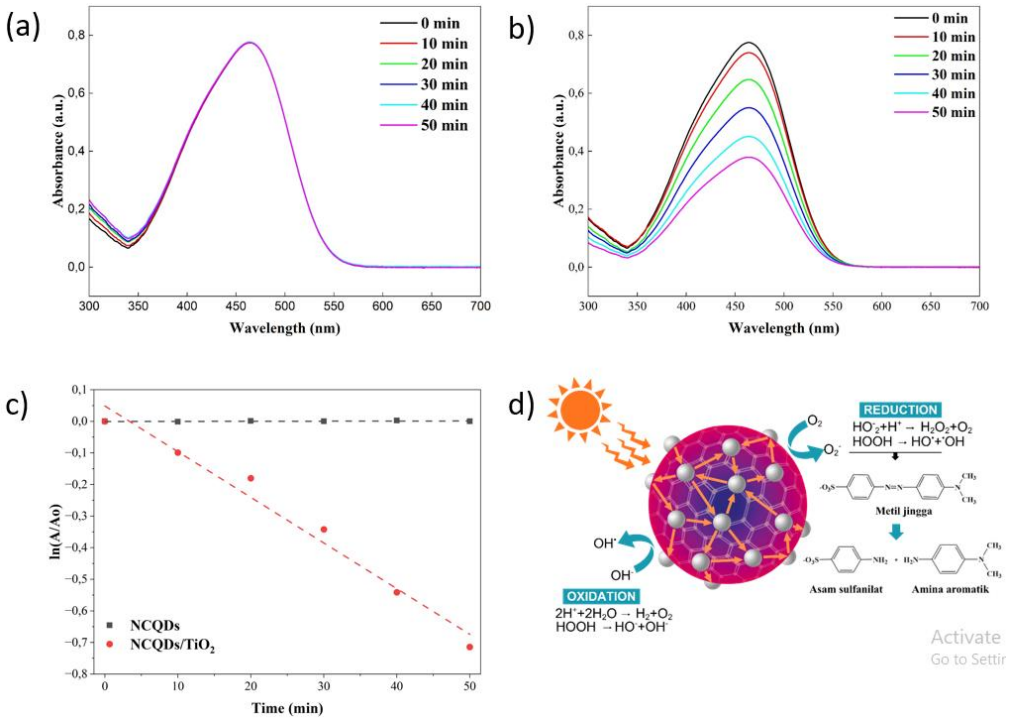

Figure 4. Photocatalytic activity of a) NCQDs; b) NCQDs/TiO_2 using MO under UV light; c) plot $\ln(A/A_0)$ vs t; and d) degradation mechanism of methyl orange.

Therefore, the superior optical profile of the 20 mg composite, combining efficient charge separation potential with the broadest visible light response among the composites, further justifies its selection for the subsequent photocatalytic degradation experiments.

The photocatalytic performance of the pristine NCQDs and the optimized NCQDs/TiO_2 composite was evaluated through the degradation of MO under visible light irradiation. The optimized composite, containing 20 mg of TiO_2 NPs, was selected for this analysis based on preliminary characterization (e.g., SEM-EDX analysis), which indicated a more homogeneous dispersion of TiO_2 NPs and favorable elemental composition compared to formulations with higher TiO_2 NPs loading (40 mg and 60 mg).

The degradation process was monitored over 50 minutes using UV-Vis spectroscopy, with the results presented in Figure 4. The control experiment utilizing only pristine NCQDs exhibited no significant photocatalytic activity. As shown in Figure 4a, the characteristic absorbance peak of MO at approximately 464 nm remained virtually unchanged throughout the 50-minute irradiation period (Absorbance ≈ 0.775). This observation indicates that the pristine NCQDs, under the given experimental conditions, are incapable of generating sufficient reactive species to degrade the MO dye.

In striking contrast, the NCQDs/TiO_2 composite demonstrated substantial photocatalytic efficacy. Figure 4b clearly illustrates a progressive decrease in the MO absorbance peak over time. The initial absorbance (A_0) of 0.775 was reduced to 0.3794 (A_t) after 50 minutes. This corresponds to a degradation efficiency of 51.05%, calculated using the formula Efficiency(%) = $((A_0 - A_t)/A_0) \times 100$. This significant reduction in absorbance confirms the composite's ability to effectively degrade the dye, a synergistic outcome of combining NCQDs with TiO_2 NPs.

To quantify the reaction rate of the photodegradation process, the experimental data were fitted to a pseudo-first-order kinetic model, which is commonly described by the equation $\ln(C_0/C_t) = kt$, where C_0 is the initial dye concentration, C_t is the concentration at time t, and k is the apparent rate constant (Prabhakaran et al., 2025). In this study, absorbance values were used as a proxy for concentration (C α A), thus the equation becomes $\ln(A_0/At) = t$.

The kinetic plot of $\ln(A/A_0)$ versus time (which is equivalent to (A_0/A) vs. time) is presented in Figure 4c. The data for the NCQDs/TiO_2 composite (red circles) yielded a strong linear

relationship, with a high coefficient of determination (R^2) of 0.97442. This confirms that the photodegradation of MO by the composite material adheres well to the pseudo-first-order kinetic model (Immanuel et al., 2025). From the linear regression, the apparent rate constant (*k*) was determined to be 0.01446 min^{-1}. Conversely, the plot for the pristine NCQDs (black squares) was nearly flat, with a slope (k) approaching zero (-2.947×10^{-5} min^{-1}) and a very low R^2 value (0.17146). The statistical analysis confirms that this slope is not significantly different from zero, reinforcing the UV-Vis data that no appreciable degradation occurred.

The enhanced photocatalytic activity of the NCQDs/TiO_2 composite, compared to its constituent parts, is attributed to a synergistic effect that promotes efficient charge separation and the generation of reactive oxygen species (ROS). The proposed mechanism is illustrated in Figure 4d. Under visible light irradiation, both components can be excited. TiO_2 NPs (a wide-bandgap semiconductor) is primarily excited by UV light, but its coupling with NCQDs can enhance its visible light response and the NCQDs known for their broad absorption spectrum can absorb visible light photons to generate electron-hole pairs (e^-/h^+) (Samir et al., 2024).

The key to the enhanced activity lies in the heterojunction formed between the NCQDs and TiO_2 NPs. Due to the favorable alignment of their band potentials, the photogenerated electrons (e^-) from the TiO_2 conduction band (or the excited NCQDs) tend to migrate to the NCQDs. The NCQDs act as an electron sink or acceptor (Zhang et al., 2021)). This process effectively separates the photogenerated electrons from the holes (h^+), significantly suppressing their rapid recombination, which is the primary limiting factor for photocatalytic efficiency (Liu et al., 2024). The homogenous dispersion of TiO_2 NPs on the NCQDs, as observed in SEM analysis, maximizes the interfacial area for this crucial charge transfer.

The electrons (e^-) accumulated on the NCQDs react with adsorbed molecular oxygen (O_2) to produce superoxide radicals ($O_2^{\bullet-}$). The holes (h^+) remaining in the valence band of TiO_2 NPs are powerful oxidizing agents. They react with water (H_2O) or hydroxide ions (OH^-) on the surface to generate highly reactive hydroxyl radicals ($OH^\bullet$). These superoxide radicals can further react to form other ROS, such as hydroperoxyl radicals ($HOO^\bullet$) and H_2O_2, which can also contribute to degradation (Waluyo et al., 2024).

As depicted in Figure 4d, these potent ROS (primarily $OH^\bullet$ and $O_2^{\bullet-}$ attack the adsorbed MO molecules. They initiate a series of oxidation and reduction reactions that cleave the dye's chromophoric azo bond (–N=N–), breaking it down into smaller, colorless organic intermediates (like sulfanilic acid and an aromatic amine) and, ultimately, promoting its mineralization into CO_2 and H_2O (Liu et al., 2024). This cleavage of the chromophore is directly responsible for the decolorization observed in the UV-Vis spectra.

In summary, the successful synthesis of the NCQDs/TiO_2 composite creates a highly efficient photocatalyst. The NCQDs serve a dual role: enhancing visible light absorption and, more importantly, acting as a charge separator to prolong the lifetime of e^-/h^+ pairs. This synergy leads to a significant increase in ROS production and, consequently, a much higher degradation rate for MO compared to pristine NCQDs.

CONCLUSION

In this study, a novel NCQDs/TiO_2 nanocomposite was successfully synthesized using a sustainable and cost-effective approach, valorizing orange peel waste as a carbon precursor for NCQDs via a one-step hydrothermal method. The influence of TiO_2 nanoparticle loading (20, 40, and 60 mg) on the material's structural, morphological, and optical properties was systematically investigated. Characterization using SEM-EDX confirmed that the 20 mg TiO_2 composite possessed the most optimal morphology, characterized by a homogeneous dispersion of TiO_2 NPs within the NCQD matrix and the highest relative carbon content. This superior structure was further corroborated by UV-Vis optical analysis, where the 20 mg sample exhibited the most favorable balance between significant absorbance quenching—indicating effective electronic coupling and charge transfer potential—and the retention of a pronounced absorption tail in the visible light region. The photocatalytic activity of the optimized 20 mg NCQDs/TiO_2 composite demonstrated a significant enhancement in the degradation of MO under visible light irradiation. The composite achieved a degradation efficiency of 51.05% within 50 minutes, whereas the pristine NCQDs control sample showed negligible catalytic activity under

identical conditions. The degradation process was found to adhere well to a pseudo-first-order kinetic model, yielding an apparent rate constant (k) of 0.01446 min^{-1}. This superior performance is unequivocally attributed to a synergistic mechanism at the NCQDs/TiO_2 heterojunction. The NCQDs serve a dual role: enhancing visible light harvesting and, more critically, acting as an electron sink to promote efficient charge separation. This process effectively suppresses the recombination of photogenerated electron-hole pairs, thereby leading to an increased production of reactive oxygen species (ROS) responsible for the cleavage and mineralization of the dye molecules. These findings conclude that the nanocomposite synthesized from orange peel waste is a promising, sustainable, and effective photocatalyst for the remediation of organic dye pollutants. Future research could be directed towards optimizing the synthesis parameters, evaluating the catalyst's long-term stability and reusability, and assessing its efficacy against a broader spectrum of persistent organic pollutants in real industrial wastewater samples.

ACKNOWLEDGMENTS

We would like to express our gratitude to Kementerian Pendidikan, Kebudayaan, Riset, dan Teknologi (Kemendikbudristek) melalui Direktorat Jenderal Pendidikan Tinggi dan Riset Republic of Indonesaia, as well as Universitas Negeri Semarang for their support in providing facilities and funding for this research.

REFERENCES

Abriyani, E., Putri, N. S., Rosidah, R. S. N., Ismanita, S. S. 2022. Analisis Kafein Menggunakan Metode Uv-Vis: Tinjauan Literatur. Jurnal Pendidikan Dan Konseling (JPDK). 4(6): 12732-12739.

Alardhi, S. M., Fiyadh, S. S., Salman, A. D., Adelikhah, M. 2023. Prediction of methyl orange dye (MO) adsorption using activated carbon with an artificial neural network optimization modeling. Heliyon. 9(1): e12888.

Aljuaid, A., Almehmadi, M., Alsaiari, A. A., Allahyani, M., Abdulaziz, O., Alsharif, A., Alsaiari, J., Saih, M., Alotaibi, R. Khan, I. 2023. g-C3N4 based photocatalyst for the efficient photodegradation of toxic methyl orange dye: recent modifications and future perspectives. Molecules. 28(7): 3199.

Aslan, M., Eskalen, H., Kavgaci, M. 2023. Carbon Quantum Dot (CQD) Nanoparticles synthesized by sucrose and urea: application as reinforcement effect on Al–Mg–Cu–Zn composite. Russian Journal of General Chemistry. 93(8): 2152-2160.

Chen, Y., Hong, C., Xu, Q., Zheng, H., Wang, C., Lu, H., Zhang, S., Du, M., Zeng, G. 2024. Visible light enhancement of biocarbon quantum-dot-decorated TiO2 for naphthalene removal. Molecules. 29(11): 2708.

Cui, L., Ren, X., Sun, M., Liu, H., Xia, L. 2021. Carbon dots: Synthesis, properties and applications. Nanomaterials. 11(12): 3419.

Dutta, S., Adhikary, S., Bhattacharya, S., Roy, D., Chatterjee, S., Chakraborty, A., Banerjee, D., Ganguly, A., Nanda, S., Rajak, P. 2024. Contamination of textile dyes in aquatic environment: Adverse impacts on aquatic ecosystem and human health, and its management using bioremediation. Journal of Environmental Management. 353: 120103.

Dong, Z., Qi, J., Yue, L., Zhou, H., Chen, L., Gu, J., He, Y., Wu, H. 2024. Biomass-based carbon quantum dots and their agricultural applications. Plant Stress. 11: 100411.

Emmanuel, S. S., Adesibikan, A. A., Opatola, E. A., Olawoyin, C. O. 2023. A pragmatic review on photocatalytic degradation of methyl orange dye pollutant using greenly biofunctionalized nanometallic materials: A focus on aquatic body. Applied organometallic chemistry. 37(7): e7108.

Harunrasjid, M. C., Aritonang, A. B., Wibowo, M. A., Ardiningsih, P. 2023. Sintesis Lapisan Tipis Ni doped-TiO2 pada Permukaan Kaca. Indonesian Journal of Chemical Analysis. 6(1): 85-96

Hu, X., Li, Y., Xu, Y., Gan, Z., Zou, X., Shi, J., Huang, X., Li, Z. Li, Y. 2021. Green One-step Synthesis of Carbon Quantum Dots from Orange Peel for Fluorescent Detection of Escherichia Coli in Milk. Food Chemistry. 339: 127775.

Immanuvel, A., Sivaranjana, P., Suresh, S., Rajini, N., Alahmadi, T. A., Sathishkannan, R.,

Rameshkumar, P., Gokulakrishnan, S. 2024. Integration of orange peel derived carbon quantum dots with TiO2 for enhanced photocatalytic degradation of brilliant green dye. Inorganic Chemistry Communications. 170: 113223.

Jayaweera, S., Yin, K., Hu, X., Ng, W. J. 2019. Facile preparation of fluorescent carbon dots for label-free detection of Fe3+. Journal of Photochemistry and Photobiology A: Chemistry. 370: 156-163.

Jubu, P.R., Danladi, E., Ndeze, U.I., Adedokun, O., Landi Jr, S., Haider, A.J., Adepoju, A.T., Yusof, Y., Obaseki, O.S., Yam, F.K. 2024. Comment about the use of unconventional Tauc plots for bandgap energy determination of semiconductors using UV–Vis spectroscopy. Results in Optics. 14: 100606.

Karaca, M., Eroglu, Z., Acışlı, O., Metin, O., Karaca, S. 2023. Boosting tetracycline degradation with an S-scheme heterojunction of N-doped carbon quantum dots-decorated TiO_2. ACS omega. 8(29): 26597-26609.

Khan, M.S., Shah, J.A., Arshad, M., Halim, S.A., Khan, A., Shaikh, A.J., Riaz, N., Khan, A.J., Arfan, M., Shahid, M., Pervez, A. 2020. Photocatalytic Decolorization and Biocidal Applications of Nonmetal Doped TiO_2: Isotherm, Kinetic Modeling and In Silico Molecular Docking Studies. Molecules. 25(19): 4468.

Kim, K. S., Zakia, M., Yoon, J., Yoo, S. I. 2019. Metal-enhanced fluorescence in polymer composite films with Au@ Ag@ SiO_2 nanoparticles and InP@ ZnS quantum dots. RSC advances. 9(1): 224-233.

Lan, D., Zhu, H., Zhang, J., Li, S., Chen, Q., Wang, C., Wu, T., Xu, M. 2022. Adsorptive removal of organic dyes via porous materials for wastewater treatment in recent decades: A review on species, mechanisms and perspectives. Chemosphere. 293: 133464.

Liu, X., Lin, Q., Zhao, L., Fang, J., Qi, J., Fan, H., Yue, X., Li, G., Qian, Y., Li, H. 2024. Wood-supported nitrogen-doped carbon quantum dot@ Cu_2O composites for efficient photocatalytic degradation of dye wastewater. Cellulose. 31(12): 7587-7600.

Malitha, M. D., Molla, M. T. H., Bashar, M. A., Chandra, D., Ahsan, M. S. 2024. Fabrication of a reusable carbon quantum dots (CQDs) modified nanocomposite with enhanced visible light photocatalytic activity. Scientific Reports. 14(1): 17976.

Mahmood, A., Shi, G., Wang, Z., Rao, Z., Xiao, W., Xie, X., Sun, J. 2021. Carbon quantum dots-TiO2 nanocomposite as an efficient photocatalyst for the photodegradation of aromatic ring-containing mixed VOCs: an experimental and DFT studies of adsorption and electronic structure of the interface. Journal of Hazardous Materials. 401: 123402.

Marpongahtun, Andriayani, Muis, Y., Gea, S., Amaturrahim, S.A., Attaurrazaq, B., Daulay, A., Salmiati, S. 2024. Biomass-derived N-doped Carbon Dots/TiO_2 for Visible-Light-Induced Degradation of Methyl Orange in Wastewater. Chemistry Africa. 7(6): 3319-3328.

Mei, A., Xu, Z., Wang, X., Liu, Y., Chen, J., Fan, J., Shi, Q. 2022. Photocatalytic materials modified with carbon quantum dots for the degradation of organic pollutants under visible light: A review. Environmental Research. 214: 114160.

Mozdbar, A., Nouralishahi, A., Fatemi, S., Talatori, F. S. 2023. The impact of Carbon Quantum Dots (CQDs) on the photocatalytic activity of TiO_2 under UV and visible light. Journal of Water Process Engineering. 51: 103465.

Nille, O. S., Patil, A. S., Waghmare, R. D., Naik, V. M., Gunjal, D. B., Kolekar, G. B., Gore, A. H. 2021. Valorization of tea waste for multifaceted applications: a step toward green and sustainable development. In Valorization of agri-food wastes and by-products. pp. 219-236. Academic Press.

Nazibudin, N. A., Zainuddin, M. F., Abdullah, C. C. 2023. Hydrothermal synthesis of carbon quantum dots: An updated review. Journal of Advanced Research in Fluid Mechechanic and Thermal Science. 101: 192-206.

Nazir, M.A., Elsadek, M.F., Ullah, S., Hossain, I., Najam, T., Ullah, S., Muhammad, N., Shah, S.S.A., Rehman, A. 2024. Synthesis of bimetallic Mn@ ZIF–8 nanostructure

for the adsorption removal of methyl orange dye from water. Inorganic Chemistry Communications. 165: 112294.

Olmos-Moya, P.M., Velazquez-Martinez, S., Pineda-Arellano, C., Rangel-Mendez, J.R. and Chazaro-Ruiz, L.F. (2022). High added value functionalized carbon quantum dots synthetized from orange peels by assisted microwave solvothermal method and their performance as photosensitizer of mesoporous TiO_2 photoelectrodes. Carbon. 187: 216-229.

Peerakiatkhajohn, P., Butburee, T., Sul, J.H., Thaweesak, S., Yun, J.H. 2021. Efficient and rapid photocatalytic degradation of methyl orange dye using Al/ZnO nanoparticles. Nanomaterials. 11(4): 1059.

Prabhakaran, P. K., Balu, S., Sridharan, G., Ganapathy, D., Sundramoorthy, A. K. 2025. Development of Eco-friendly CQDs/TiO_2 nanocomposite for enhanced photocatalytic degradation of methyl orange dye. Engineering Research Express. 7(1): 015002.

Putro, P. A., Roza, L., Isnaeni, I. 2018. Precursor concentration effect on optical properties of carbon dots from Cassava's peels. Journal of Physics: Theories and Applications. 2(2): 43-52.

Rahman, Q.I., Ali, A., Ahmad, N., Lohani, M.B., Mehta, S.K., Muddassir, M. 2020. Synthesis and characterization of CuO rods for enhanced visible light driven dye degradation. Journal of Nanoscience and Nanotechnology. 20(12): 7716-7723.

Remli, U. R. R. P., Aziz, A. A. 2020. Photocatalytic degradation of methyl orange using Carbon Quantum Dots (CQDs) derived from watermelon rinds. IOP Conference Series: Materials Science and Engineering. IOP Publishing.

Sadeghi-Chahnasir, F., Amiripour, F. and Ghasemi, S. 2024. Orange Peel-derived Carbon Dots/Cu-MOF Nanohybrid for Fluorescence Determination of L-ascorbic Acid and Fe^{3+}. Analytica Chimica Acta. 1287: 342066.

Samir, M., Agour, A. M., Ismail, Z., Nageh, H., Abdellatif, S. O. 2023The impact of N-doped carbon quantum dots on dye-sensitized solar cells operating under diffused-and low-light intensity. IEEE Journal of photovoltaics. 14(2): 253-259.

Su, H., Wang, J., Yan, L. 2019. Homogeneously synchronous degradation of chitin into carbon dots and organic acids in aqueous solution. ACS Sustainable Chemistry & Engineering. 7(22): 18476-18482.

Surendran, P., Lakshmanan, A., Vinitha, G., Ramalingam, G., Rameshkumar, P. 2020. Facile preparation of high fluorescent carbon quantum dots from orange waste peels for nonlinear optical applications. Luminescence. 35(2): 196-202.

Song, F., Sun, H., Ma, H., Gao, H. 2022. Porous TiO2/carbon dot nanoflowers with enhanced surface areas for improving photocatalytic activity. Nanomaterials. 12(15): 2536.

Tahir, Z., Khan, M.I., Ashraf, U., Adan, I.R.D.N., Mubarik, U. 2023. Industrial application of orange peel waste; a review. International Journal of Agriculture and Biosciences. 12(2): 71-76.

Thangaraj, B., Solomon, P.R., Chuangchote, S., Wongyao, N., Surareungchai, W. 2021. Biomass-derived Carbon Quantum Dots–A Review. Part 1: Preparation and Characterization. ChemBioEng Reviews. 8(4): 265-301.

Toro, R.G., Diab, M., de Caro, T., Al-Shemy, M., Adel, A. Caschera, D. 2020. Study of the effect of titanium dioksida hydrosol on the photocatalytic and mechanical properties of paper sheets. Materials. 13(6): 326.

Waluyo, R., Hadju, A., Rati, Y., Marlina, R., Darma, Y. 2024. Facile synthesis of Pangium edule kernel biomass-derived NCQDs/TiO_2/PVA nanocomposite film for visible light-assisted methylene blue reduction. Biomass and Bioenergy. 180: 106992.

Xie, C., Fan, T., Wang, A., Chen, S. L. 2018. Enhanced visible-light photocatalytic activity of a TiO_2 membrane-assisted with N-doped carbon quantum dots and SiO_2 opal photonic crystal. Industrial & Engineering Chemistry Research. 58(1): 120-127.

Zakia, M., Yoo, S. I. 2022. Enhanced photocatalytic activity of TiO_2 nanoparticles immobilized on porous-sulfonated polystyrene microspheres

through multiple scattering process. Macromolecular Research. 30(9): 677-683.

Zhang, D., Chen, L., Xu, M., Feng, G., Zhang, B., Zhang, H., Yang, C., Yu, Q., Wang, L. 2022. Visible-light responsive PVDF/carbon sphere@ TiO_2 membrane for dye scavenging and bacteria inactivation. Applied Surface Science. 605: 154755.

Zhang, J., Liu, Q., Wang, J., He, H., Shi, F., Xing, B., Jia, J., Huang, G., Zhang, C. 2021. Facile preparation of carbon quantum dots/TiO_2 composites at room temperature with improved visible-light photocatalytic activity. Journal of Alloys and Compounds. 869: 159389.